Circuit Extraction via Time-Domain Vector Fitting

Circuit Extraction via Time-Domain Vector Fitting

S. Grivet-Talocia, F. G. Canavero, I. S. Stievano, I. A. Maio
Dipartimento di Elettronica, Politecnico di Torino,
Corso Duca degli Abruzzi 24, 10129, Torino, Italy
Email: stefano.grivet@polito.it

Abstract— **This paper introduces a new algorithm for the automatic synthesis of SPICE-ready equivalent circuits of complex multiport lumped interconnect structures. The method is named Time-Domain Vector Fitting (TD-VF) due to its analogy to the well-known Vector Fitting algorithm, which operates in frequency domain. The TD-VF computes a rational approximation of the transfer matrix for the structure under modeling using as raw data its transient port responses to suitable excitations. These include, e.g., the case of transient port scattering responses as typically obtained by full-wave electromagnetic solvers based on the Finite-Differences Time-Domain (FDTD) or Finite Integration (FIT) methods. The TD-VF algorithm works entirely in the time domain, without requiring any knowledge of the frequency-domain responses. This allows direct processing of possibly truncated transient responses, therefore allowing for short full-wave simulations. This paper shows that the accuracy level achiavable by TD-VF is excellent. Hence, passivity can be enforced a posteriori using the spectral properties of associated Hamiltonian matrices. Several examples of package, connectors, and discontinuities are provided as illustration.**

I. Introduction

The signal integrity of electronic systems may be strongly affected by discontinuities in the signal propagation paths. Such discontinuities can be vias and via arrays, bends, junctions, connectors, etc. A careful assessment requires a proper modeling of such structures in order to be able to reproduce their effects on the signals. This modeling procedure should take into account geometry and material properties, thus requiring a complex full-wave electromagnetic analysis. Instead of applying this costly analysis to the entire system, we consider its subparts separately. Each sub-structure is characterized via full-wave analysis (and/or by direct measurement). The port responses that are obtained are used to derive suitable macromodels of each sub-structure. Finally, all the macromodels are translated into an equivalent circuit, in order to connect them and to run a system-level transient analysis using a standard SPICE-like circuit solver. This analysis can be finalized to investigate couplings, to compute eye diagrams for safe transmission, etc.

The macromodeling problem has received much attention in the recent literature, and several macromodeling techniques are now available (see, e.g., Refs. [1], [2], [7], [8]). Each of these techniques is tailored to the specific form in which the structure under investigation is characterized. We focus here on linear macromodeling from transient port responses, and we present a new macromodeling technique that we denote Time-Domain Vector Fitting (TD-VF). The algorithm is an extension of the well-known standard Vector-Fitting (VF) technique [8], whose accuracy and efficiency is widely recognized. Standard VF operates entirely in frequency domain, providing rational approximations of transfer functions starting from frequency-domain samples. Conversely, the proposed TD-VF technique produces rational approximations directly from transient input/output responses. A specific application where this approach is convenient is the equivalent circuit extraction for three-dimensional interconnect structures (like, e.g., electronic packages or connectors), that are characterized using a full-wave electromagnetic solver based, e.g., on the Finite-Difference Time-Domain (FDTD), Finite Integration (FIT), or transient Partial Element Equivalent Circuit (PEEC) methods. Due to the high computational cost, it is desirable to terminate the full-wave analysis before all transients have extinguished, thus obtaining truncated time responses. The presented algorithm is ideally suited for this type of native data, whereas a frequency-domain approach would not be feasible. In addition, in order to handle the large number of port responses in case of a high ports count, a decomposition strategy is devised to compute partial macromodels from separate subsets of port responses, and to assemble them into a global state-space realization of the macromodel.

The synthesis of a SPICE equivalent circuit from state-space equations is conventional. However, we remark that passivity should be tested and enforced before performing this synthesis. The macromodels generated by TD-VF are either passive or nearly-passive due to the excellent accuracy of the macromodeling algorithm. Therefore, passivity can be enforced a posteriori. We use here a recently-developed algorithm based on spectral perturbations of associated Hamiltonian matrices, which leads to a necessary and sufficient passivity test and to an iterative passivity compensation procedure that ensures a minimal impact on the macromodel accuracy. Full derivation, theorem proofs, and details can be found in [5], [6]. The combination of TD-VF and Hamiltonian-based passivity tools leads to a powerful macromodeling methodology that has been verified on several applications.

II. Time-Domain Vector Fitting

We consider a multiport structure with an arbitrary number P of ports. Input and output vectors are denoted as $\boldsymbol{x}$ and $\boldsymbol{y}$, respectively. Usually, a transient characterization of such a multiport structure is obtained by exciting one port at the time and computing/measuring the responses at all ports. As a result, the raw data set is a matrix of response waveforms $y_{ij}(t)$ at port (i), due to an excitation source $x_j(t)$ located at

0-7803-8443-1/04/$20.00 © IEEE.

port (j). If we denote with $\boldsymbol{H}(s)$ the transfer matrix of the structure, we have

$$\begin{aligned} \boldsymbol{Y}(s) &= \boldsymbol{H}(s)\boldsymbol{X}(s)\,, \\ y_{ij}(t) &\simeq \mathcal{L}^{-1}\{H_{ij}(s)\} * x_j(t)\,, \quad i,j=1,\ldots,P\,, \end{aligned} \tag{1}$$

where $\mathcal{L}^{-1}$ is the inverse Laplace operator and $*$ denotes convolution. We remark that this type of data set is the natural outcome of time-domain full-wave electromagnetic solvers (transient scattering waveforms being the typical format). The objective is the derivation of a rational approximation

$$\boldsymbol{H}(s) \simeq \boldsymbol{H}_\infty + \sum_{n=1}^{N} \frac{\boldsymbol{R}_n}{s-p_n}\,, \tag{2}$$

since this can be easily translated into an equivalent circuit.

Since the entire dataset of port responses may be very large, we first split them into separate subsets. Let

$$\boldsymbol{x}_k = \boldsymbol{P}_k\boldsymbol{x}\,, \qquad \boldsymbol{y}_k = \boldsymbol{Q}_k\boldsymbol{y}\,, \qquad k=1,\ldots,K \tag{3}$$

collect some P_k pairs of input-output responses selected from the global set. Matrices $\boldsymbol{P}_k$ and $\boldsymbol{Q}_k$ are $P_k \times P$ port selectors having a single unitary entry in each row with all the other entries vanishing. These vectors of partial responses can be related in the Laplace domain via

$$\boldsymbol{Y}_k(s) = \boldsymbol{H}_k(s)\boldsymbol{X}_k(s)\,, \tag{4}$$

where $\boldsymbol{H}_k(s)$ is diagonal and stores the entries of the global transfer matrix $\boldsymbol{H}(s)$ corresponding to the selected port responses. It is assumed that all input-output pairs appear only once in this subdivision for some index k. Therefore, we can easily show that

$$\boldsymbol{H}(s) = \sum_{k=1}^{K} \boldsymbol{Q}_k^T \boldsymbol{H}_k(s)\boldsymbol{P}_k\,. \tag{5}$$

In the following we will first look for a partial macromodel for each $\boldsymbol{H}_k(s)$ in the form

$$\boldsymbol{H}_k(s) \simeq \boldsymbol{H}_{k,\infty} + \sum_{n=1}^{N_k} \frac{\boldsymbol{R}_{k,n}}{s-p_{k,n}}\,, \tag{6}$$

with diagonal $\boldsymbol{H}_{k,\infty}$ and $\boldsymbol{R}_{k,n}$. Then, we will use (5) to recover the global macromodel for the entire structure.

The identification of the unknown poles, residues and direct coupling constants in (6) from the set of time-domain responses is performed here by the Time-Domain Vector Fitting (TD-VF) algorithm [3], [4]. This is a time-domain reformulation of the well-known Vector Fitting (VF) method [8], which operates in frequency domain. The main steps of the TD-VF algorithm are summarized in the following paragraphs.

We first introduce, as for standard VF [8], a scalar weight function

$$\sigma_k(s) = 1 + \sum_{n=1}^{N_k} \frac{r_{k,n}}{s-q_{k,n}} = \frac{\prod_{n=1}^{N_k}(s-z_{k,n})}{\prod_{n=1}^{N_k}(s-q_{k,n})} \tag{7}$$

with fixed (initial) poles $\{q_{k,n}\}$ and unknown residues $\{r_{k,n}\}$. This function is used to enforce the following condition,

$$\sigma_k(s)\boldsymbol{H}_k(s) \simeq \boldsymbol{M}_{k,\infty} + \sum_{n=1}^{N_k} \frac{\boldsymbol{M}_{k,n}}{s-q_{k,n}}\,. \tag{8}$$

According to this condition, the right-hand-side must have the same poles $\{q_{k,n}\}$ as the weight function, a cancellation between the zeros $\{z_{k,n}\}$ of $\sigma_k(s)$ and the poles $\{p_{k,n}\}$ of $\boldsymbol{H}_k(s)$ must occur. Therefore (8) is first solved for the unknown residues $\{r_{k,n}\}$, then the zeros $\{z_{k,n}\}$ are computed using standard techniques [8]. This procedure leads to the macromodel poles $p_{k,n} = z_{k,n}$.

In order to use transient responses in the poles identification, we reformulate (8) in time domain by applying it to the input signals $\boldsymbol{X}_k(s)$ and by using inverse Laplace transform. We get

$$\boldsymbol{y}_k(t) \simeq \boldsymbol{M}_{k,\infty}\boldsymbol{x}_k + \sum_{n=1}^{N_k} \boldsymbol{M}_{k,n}\boldsymbol{x}_{k,n}(t) - \sum_{n=1}^{N_k} r_{k,n}\boldsymbol{y}_{k,n}(t)\,, \tag{9}$$

where the transient waveforms

$$\begin{aligned} \boldsymbol{x}_{k,n}(t) &= \int_0^t e^{q_{k,n}(t-\tau)}\boldsymbol{x}_k(\tau)d\tau\,, \\ \boldsymbol{y}_{k,n}(t) &= \int_0^t e^{q_{k,n}(t-\tau)}\boldsymbol{y}_k(\tau)d\tau \end{aligned} \tag{10}$$

are convolutions resulting from inverse Laplace transform of each partial fraction in the expansions (7)-(8). These waveforms are easily obtained by applying a suitable discretization of the convolution integrals. We remark that due to the exponential nature of the convolution kernels, a fast implementation based on recursive convolutions, i.e., digital IIR filtering, is used [3], [4].

The condition (9) is enforced in least squares sense using raw and filtered input/output sequences. Solution of this linear system returns the residues $\{r_{k,n}\}$ of the weight function, which in turn are used as in standard VF to compute its zeros $\{z_{k,n}\}$, and consequently the poles $\{p_{k,n}\}$ of the sought approximation. Once these poles are known, the residues $\boldsymbol{R}_{k,n}$ and the direct coupling matrix $\boldsymbol{H}_{k,\infty}$ in (6) are computed by solving another linear least squares problem,

$$\boldsymbol{y}_{k,n}(t) \simeq \boldsymbol{H}_{k,\infty}\boldsymbol{x}_k(t) + \sum_{n=1}^{N_k} \boldsymbol{R}_{k,n}\widehat{\boldsymbol{x}}_{k,n}(t)\,, \tag{11}$$

with $\widehat{\boldsymbol{x}}_{k,n}(t)$ defined as in (10) with $\{q_{k,n}\}$ replaced by the estimated poles $\{p_{k,n}\}$. As a final step, the poles/residues representation (6) is translated by standard techniques into an equivalent state-space representation

$$\left\{ \begin{array}{rcl} \frac{d}{dt}\boldsymbol{w}_k(t) &=& \boldsymbol{A}_k\boldsymbol{w}_k(t) + \boldsymbol{B}_k\boldsymbol{x}_k(t) \\ \boldsymbol{y}_k(t) &=& \boldsymbol{C}_k\boldsymbol{w}_k(t) + \boldsymbol{D}_k\boldsymbol{x}_k(t) \end{array} \right. \tag{12}$$

This representation allows to construct a state-space representation for the macromodel of the entire structure by tiling the

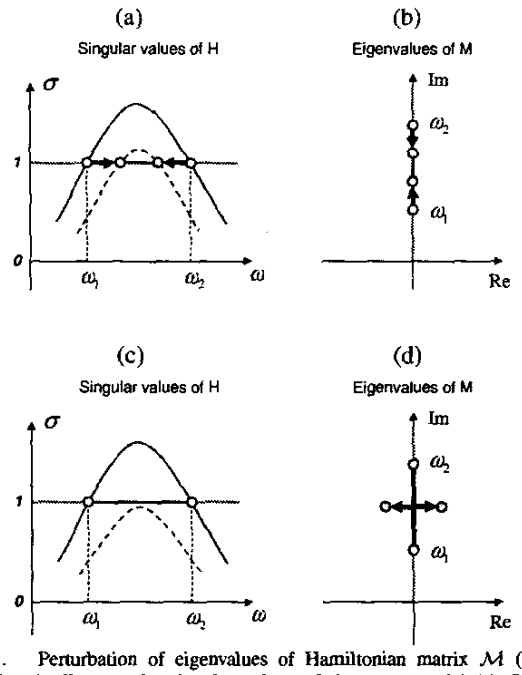

Fig. 1. Perturbation of eigenvalues of Hamiltonian matrix $\mathcal{M}$ (b) and its induced effect on the singular values of the macromodel (a). Iterative application leads to displacement of the eigenvalues off the imaginary axis (d) and consequently to passivity enforcement (c).

partial state matrices as basic blocks into the global matrices below

$$\begin{cases} \frac{d}{dt}\boldsymbol{w}(t) &= \boldsymbol{A}\boldsymbol{w}(t) + \boldsymbol{B}\boldsymbol{x}(t) \\ \boldsymbol{y}(t) &= \boldsymbol{C}\boldsymbol{w}(t) + \boldsymbol{D}\boldsymbol{x}(t) \end{cases} \tag{13}$$

This is performed using the port selector matrices in (5). Note that the resulting state matrices are possibly large but very sparse by construction.

The resulting macromodel is usually characterized by excellent accuracy. It is stable by construction. However, it might not be passive since it was identified by a sequence of least squares solutions that do not guarantee passivity a priori. Since a non-passive macromodel can lead to unstable solutions when its terminations are changed, passivity must be checked and enforced.

III. Passivity Characterization and Compensation

We recall that passivity for the adopted scattering representation requires that all singular values of the transfer matrix be bounded by one. Here we check this condition using a purely algebraic criterion based on the so-called Hamiltonian matrix. This matrix is defined for the scattering representation as

$$\mathcal{M} = \begin{pmatrix} \boldsymbol{A} - \boldsymbol{B}\boldsymbol{R}^{-1}\boldsymbol{D}^T\boldsymbol{C} & -\boldsymbol{B}\boldsymbol{R}^{-1}\boldsymbol{B}^T \\ \boldsymbol{C}^T\boldsymbol{S}^{-1}\boldsymbol{C} & -\boldsymbol{A}^T + \boldsymbol{C}^T\boldsymbol{D}\boldsymbol{R}^{-1}\boldsymbol{B}^T \end{pmatrix}, \tag{14}$$

with $\boldsymbol{R} = (\boldsymbol{D}^T\boldsymbol{D} - \boldsymbol{I})$ and $\boldsymbol{S} = (\boldsymbol{D}\boldsymbol{D}^T - \boldsymbol{I})$. Under some technical conditions that are always verified for the particular form of macromodel here considered [6], the existence of purely imaginary eigenvalues of this matrix can be related to the existence of passivity violations of the macromodel. In particular, one of the singular values of the macromodel reaches the threshold value $\gamma = 1$ at a frequency ω_0 if and only if $j\omega_0$ is an eigenvalue of $\mathcal{M}$. This condition can be applied to detect very precisely the frequency bands where passivity violations occur. Details of this procedure can be found in [5], [6].

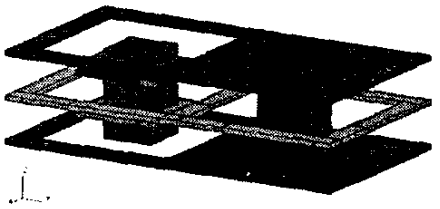

Fig. 2. Single via structure (courtesy by Dr. Ruehli, IBM)

If some violations are found, a procedure based on first-order perturbations is applied in order to eliminate them. This is achieved by perturbing the imaginary eigenvalues of the Hamiltonian matrix and forcing them to move off the imaginary axis as sketched in Figure 1, thus ensuring passivity. Each imaginary eigenvalue is displaced by an amount $\Delta\omega_i$, determined on the basis of the location of the violation bands. This displacement is enforced by computing a suitable correction term $\boldsymbol{dC}$ for the state matrix $\boldsymbol{C}$. Using a first-order analysis, this correction term is related linearly to the the set of eigenvalue perturbations $\Delta\omega_i$, leading to a simple underdetermined linear least squares system to be solved. This system can be expressed in a compact matrix form as

$$\boldsymbol{Z}\,\mathrm{vec}(\boldsymbol{dC_k}) = \boldsymbol{r}, \qquad \min||\mathrm{vec}(\boldsymbol{dC_k})||_2 \tag{15}$$

where each row corresponds to an imaginary eigenvalues to be perturbed by the amount collected in $\boldsymbol{r}$. The operator $\mathrm{vec}(\cdot)$ stacks the columns of its matrix argument, and the vector of unknowns is defined as

$$\boldsymbol{dC_k} = \boldsymbol{dC}\,\boldsymbol{K}^T. \tag{16}$$

Matrix $\boldsymbol{K}$ denotes the Cholesky factor

$$\boldsymbol{W} = \boldsymbol{K}^T\boldsymbol{K}, \tag{17}$$

of the controllability Gramian

$$\boldsymbol{W} = \int_0^\infty \exp\{\boldsymbol{A}t\}\boldsymbol{B}\boldsymbol{B}^T\exp\{\boldsymbol{A}^Tt\}\,\mathrm{d}t, \tag{18}$$

which can be computed as the unique symmetric and positive definite solution of the Lyapunov equation

$$\boldsymbol{A}\boldsymbol{W} + \boldsymbol{W}\boldsymbol{A}^T = -\boldsymbol{B}\boldsymbol{B}^T. \tag{19}$$

These definitions, together with the selection of the minimum norm solution in (15), allow to compute the perturbation by ensuring the minimal impact (at each iteration) on the accuracy of the macromodel. In fact, it can be shown that the induced perturbation $\boldsymbol{dh}$ on the matrix of impulse responses of the macromodels can be expressed as

$$\sum_{i,j=1}^{p}\int_0^\infty |(dh)_{i,j}(t)|^2\,\mathrm{d}t = ||\mathrm{vec}(\boldsymbol{dC_k})||_2^2. \tag{20}$$

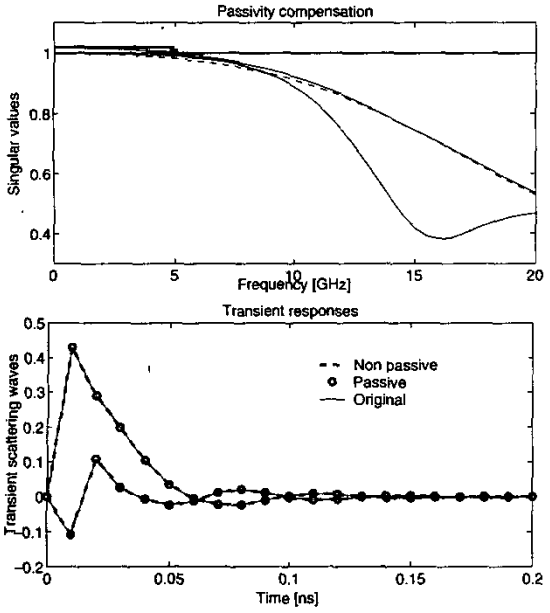

Fig. 3. Top: singular values for the non-passive macromodel (solid lines) and for the passive macromodel (dashed lines). Bottom: transient scattering responses (y_{11}: reflected, y_{21}: transmitted).

A summary of the passivity compensation algorithm is as follows

Algorithm 1: (passivity compensation)
Set $m = 0$ and $\boldsymbol{C}_0 = \boldsymbol{C}$;
Compute the set Ω of imaginary eigenvalues of $\mathcal{M}$
Repeat
Increase the iteration count $m := m + 1$;
Determine the perturbation $\boldsymbol{r}$, see [6]
Solve (15) and compute $d\boldsymbol{C}_m$ using (16);
Update the state matrix $\boldsymbol{C}_m = \boldsymbol{C}_{m-1} + d\boldsymbol{C}_m$;
Re-compute Ω
Until Ω is empty.
Further details can be found in [5], [6].

IV. Examples

The first example is a single via interconnect crossing a solid metal plane (Fig. 2). Two ports are defined between the vertical conductor and top/bottom ground planes. The structure has been meshed and analyzed via the Partial Element Equivalent Circuit (PEEC) method. A time-domain full-wave formulation has been adopted to obtain the scattering port responses (referenced to 50Ω loads) to a unitary triangle pulse excitation with a 10 ps rise and fall time. These responses have been processed by TD-VF using a 5-pole approximation. The resulting macromodel is characterized by a small passivity violation, which has been corrected by the Hamiltonian-based algorithm (Fig. 3, top panel). The three sets of transient responses (original, non-passive macromodel, passive macromodel) are depicted in the bottom panel of Fig. 3, showing excellent

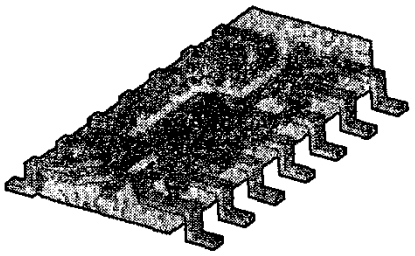

Fig. 4. SOIC-14 package

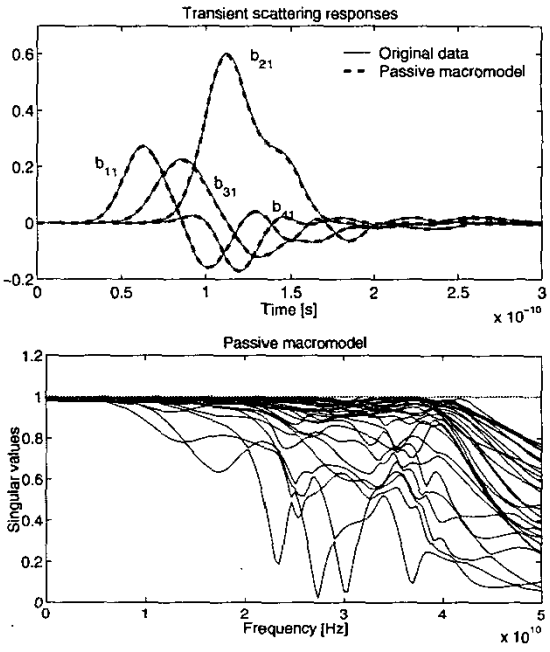

Fig. 5. Top: some responses of the passive macromodel for the SOIC-14 package compared to the raw FDTD responses. Bottom: singular values of the passive macromodel.

accuracy. On this scale, almost no difference is visible between the raw data and the two macromodel responses.

The second example is a commercial 14-pin package depicted in Fig. 4. The structure has $p = 28$ ports, half being defined between a corresponding pin and the printed circuit board on which the package is mounted, and half being defined between the bonding pad on the included die and the reference plane below the die itself. The structure has been meshed and analyzed with a full-wave electromagnetic solver based on the Finite-Difference Time-Domain (FDTD) method, obtaining a set of 28×28 transient scattering responses to Gaussian pulse excitation having a 30 GHz frequency bandwidth. The combination of TD-VF and Hamiltonian-based algorithms has been applied to obtain a passive macromodel. Some of the responses are depicted in the top panel of Fig. 5, showing excellent accuracy. The bottom panel of Fig. 5 depicts the frequency-dependent distribution of the singular values for the

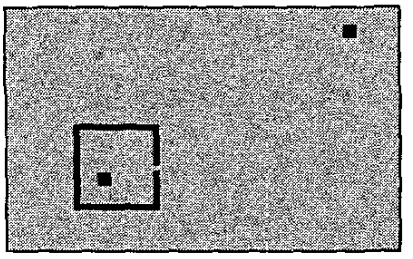

Fig. 6. Segmented power bus structure. See text for details.

model transfer (scattering) matrix. All these singular values are below 1 at all frequencies, as required by the standard passivity conditions. Note also that the distribution of the singular values is very close to 1 throughout the modeling bandwidth, since the full-wave simulation did not include any losses in both metal and dielectric.

The last example we investigate is the power/ground structure depicted in Fig. 6. A 16cm x 10cm PCB with thickness 1.4 mm is considered. For isolation purposes a power island has been cut. The dimension of the power island is 30 mm x 30 mm; the gap width (thick black line in the figure) is 2.5 mm; the width of the metal connecting the two power areas is also 2.5 mm. The two ports are depicted by small squares in the figure, one being located (port n. 1) at (40; 30) and the other (port n. 2) at the point (140; 90) (units are in mm and represent x- and y-direction, respectively). The structure has been meshed and analyzed via a full-wave electromagnetic solver based on the Finite-Integration method [9]. All ports are defined using a 50Ω reference load. The raw dataset consists therefore of a 2×2 matrix of transient scattering responses due to Gaussian pulse excitation having a 3 GHz frequency bandwidth at the -20 dB level. Due to the geometry of the structure, the electromagnetic energy remains trapped for a long time between the two metal planes, exciting the board resonances. As a result, the transient waveforms exhibit a long transient. In order to let this transient vanish so that FFT can reliably used to compute the frequency-domain scattering matrix, a long simulation time would be required (up to 1000 ns). However, we stopped the transient simulation after 100 ns (i.e., 10% of this minimum time) and we used the truncated waveforms for the estimation of the macromodel using the TD-VF algorithm. A total number of 80 poles were used for the macromodel in order to capture all the resonances within the bandwidth of interest. The macromodel resulted non-passive after the Hamiltonian-based test, as illustrated in Fig. 7, top panel. After 15 iterations of the Hamiltonian-based passivity compensation algorithm a new passive macromodel was obtained. The distribution of its frequency-dependent singular values is depicted in the bottom panel of Fig. 7, showing that all singular values are uniformly bounded by one.

The transient responses of the passive macromodel are

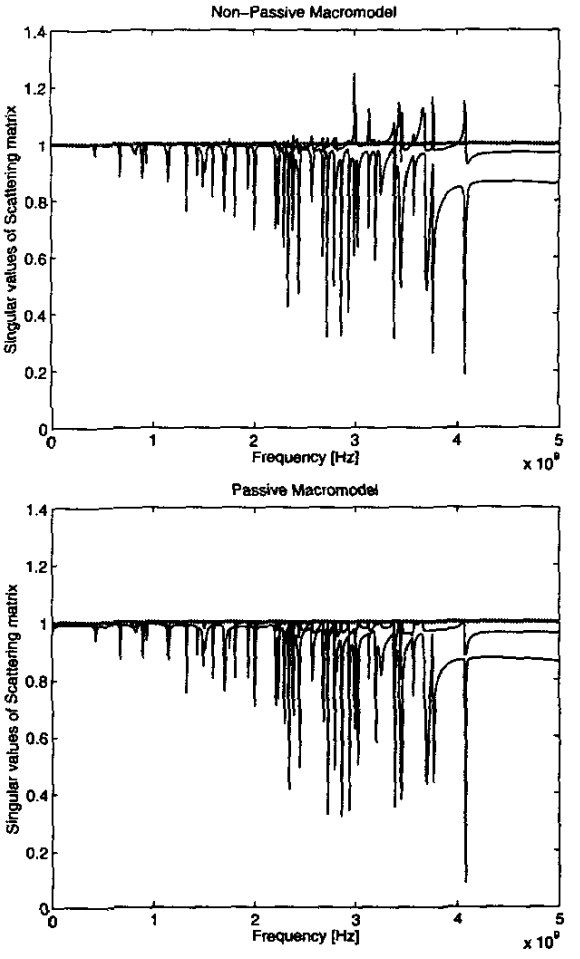

Fig. 7. Passivity compensation for the PCB power bus of Fig. 6. The singular values are plotted versus frequency for the non-passive macromodel (top panel) and for the passive macromodel (bottom panel).

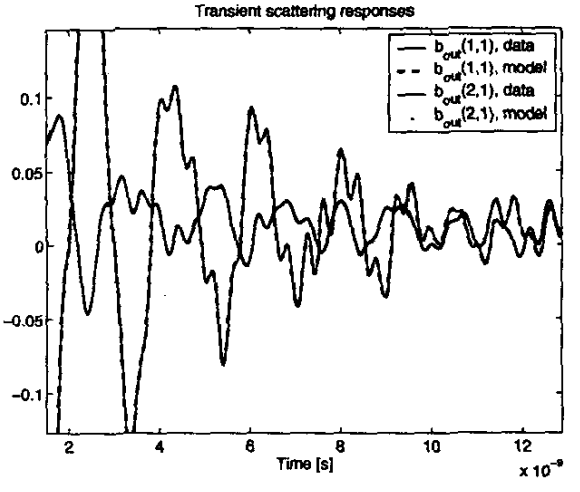

Fig. 8. Selected transient responses for the macromodel of the PCB power bus of Fig. 6. The responses of the passive macromodel are compared to the original transient data used for its identification.

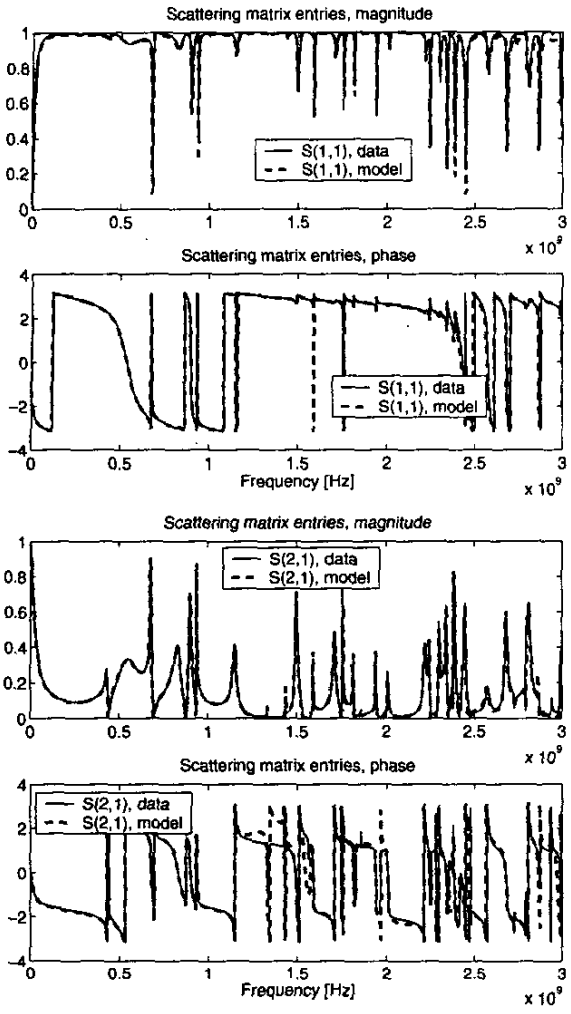

Fig. 9. Scattering matrix entries for the PCB power bus of Fig. 6. The responses of the passive macromodel are compared to the corresponding scattering matrix elements obtained by full-wave simulation.

compared in Fig. 8 to the raw dataset obtained by the full-wave solver and used for the TD-VF identification. This figure shows that, as expected, a very good accuracy is mantained even after the passivity enforcement stage. As a final check, we have computed via FFT the frequency-domain scattering matrix using the transient waveforms obtained by the long complete simulation (up to 1000 ns). The frequency responses of the macromodel are compared to these reference data in Fig. 9. Apart from a marginal deviation near the edge of the modeling bandwidth, a very good agreement is evident.

This example shows that the TD-VF algorithm combined with Hamiltonian-based passivity compensation can be very useful in modeling structures characterized by strong resonances, since truncated transient responses can be used for the model identification.

V. Conclusion

This paper presented a new macromodeling technique that works entirely in the time domain. A complete set of transient responses of the structure under investigation to given stimuli constitutes the raw dataset used for the identification of a lumped macromodel, which can be synthesized using standard techniques into a SPICE-ready subcircuit for system-level Signal Integrity analysis. This method is applicable whenever frequency-domain data are unavailable or difficult to compute. An example can be highly resonant structures characterized by slowly decaying transients. The computational core of the technique is the Time-Domain Vector Fitting algorithm, here formulated in a partitioned form enabling the macromodeling of structures with possibly many ports. In addition, passivity is checked and enforced a posteriori using spectral perturbation of associated Hamiltonian matrices.

Acknowledgment

The Authors are grateful to Dr. Ruehli of IBM for providing the data used for some of the examples. This work is supported in part by the Italian Ministry of University (PRIN grant #2002093437), and in part by CERCOM, Politecnico di Torino.

References

[1] M. Celik, L. Pileggi, A. Obadasioglu, *IC Interconnect Analysis*, Kluwer, 2002.

[2] S. Grivet-Talocia, I. S. Stievano, I. A. Maio, and F. G. Canavero, "Time-domain and frequency-domain macromodeling: application to package structures," in *IEEE International Symposium on EMC, Boston, MA*, pp. 570–574, August 18–22 2003.

[3] S. Grivet-Talocia, "The Time-Domain Vector Fitting Algorithm for Linear Macromodeling", *AEU Int. J. Electron. Commun.*, in press.

[4] S. Grivet-Talocia, "Package Macromodeling via Time-Domain Vector Fitting", *IEEE Microwave and Wireless Components Letters*, pp. 472–474, vol. 13, n. 11, November, 2003.

[5] S. Grivet-Talocia, "Enforcing Passivity of Macromodels via Spectral Perturbation of Hamiltonian Matrices" , *7th IEEE Workshop on Signal Propagation on Interconnects (SPI), Siena (Italy)*, pp. 33-36, May 11-14, 2003

[6] S. Grivet-Talocia, "Passivity enforcement via perturbation of Hamiltonian matrices", *IEEE Trans. CAS-I*, 2004, in press.

[7] M. Nakhla and R. Achar, "Simulation of High-Speed Interconnects", *Proc. IEEE*, May 2001, Vol. 89, No. 5, pp. 693–728.

[8] B. Gustavsen, A. Semlyen, "Rational approximation of frequency responses by vector fitting", *IEEE Trans. Power Delivery*, Vol. 14, July 1999, pp. 1052–1061.

[9] *CST Microwave Studio Manual*, Computer Simulation Technology GmbH, Germany, 2003 (www.cst.de).